Universal robotic gripper based on the jamming of granular material

Eric Brown[a,1], Nicholas Rodenberg[a], John Amend[b], Annan Mozeika[c], Erik Steltz[c], Mitchell R. Zakin[d], Hod Lipson[b], and Heinrich M. Jaeger[a]

[a]James Franck Institute and Department of Physics, University of Chicago, Chicago, IL 60637; [b]School of Mechanical and Aerospace Engineering, Cornell University, Ithaca, NY 14853; [c]iRobot G and I Research, 8 Crosby Drive, Bedford, MA 01730; and [d]Defense Advanced Research Projects Agency, 3701 North Fairfax Drive, Arlington, VA 22203

Edited by Daniel Meiron, Cal Tech, and accepted by the Editorial Board September 17, 2010 (received for review March 16, 2010)

Gripping and holding of objects are key tasks for robotic manipulators. The development of universal grippers able to pick up unfamiliar objects of widely varying shape and surface properties remains, however, challenging. Most current designs are based on the multifingered hand, but this approach introduces hardware and software complexities. These include large numbers of controllable joints, the need for force sensing if objects are to be handled securely without crushing them, and the computational overhead to decide how much stress each finger should apply and where. Here we demonstrate a completely different approach to a universal gripper. Individual fingers are replaced by a single mass of granular material that, when pressed onto a target object, flows around it and conforms to its shape. Upon application of a vacuum the granular material contracts and hardens quickly to pinch and hold the object without requiring sensory feedback. We find that volume changes of less than 0.5% suffice to grip objects reliably and hold them with forces exceeding many times their weight. We show that the operating principle is the ability of granular materials to transition between an unjammed, deformable state and a jammed state with solid-like rigidity. We delineate three separate mechanisms, friction, suction, and interlocking, that contribute to the gripping force. Using a simple model we relate each of them to the mechanical strength of the jammed state. This advance opens up new possibilities for the design of simple, yet highly adaptive systems that excel at fast gripping of complex objects.

stress-strain | packing density | friction | suction | interlocking

Tasks that appear simple to humans, such as picking up objects of varying shapes, can be vexingly complicated for robots. Secure gripping not only requires contacting an object, but also preventing potential slip while the object is moved. Slip can be prevented either by friction from contact pressure or by exploiting geometric constraints, for example by placing fingers around protrusions or into the opening provided by the handle of a cup. For reliable robotic gripping, the standard design approach is based on a hand with two or more fingers (1–5), and typically involves a combination of visual feedback and force sensing at the fingertips. A large number of optimization schemes for finger placement as well as the use of compliant materials for adaptive grasping have been discussed (5–15). Given the evolutionary success of the multifingered hand in animals, this approach clearly has many advantages. However, it requires a central processor or brain for a multitude of decisions, many of which have to be made before the hand even touches the object, for example about how wide to spread the fingers apart. Therefore, a multifingered gripper not only is a complex system to build and control, but when confronted with unfamiliar objects it may require learning the shape and stiffness of the object.

The focus of this work is on the problem of gripping, not manipulation, and seeks to offload system complexities such as tactile sensing and computer vision onto unique mechanical design. This approach replaces individual fingers by a material or interface that upon contact molds itself around the object. Such a gripper is universal in the sense that it conforms to arbitrary shapes and is passive in that all shape adaptation is performed autonomously by the contacting material and without sensory feedback. This passive process reduces the number of elements to be controlled and therefore can have advantages in terms of reliability, cost, and gripping speed. So far, however, passive universal grippers have remained largely unexplored. An early snake-like gripper by Hirose (16) employed a system of joints and pulleys with a single actuator. A few designs have envisioned systems where moveable jaws with highly compliant surfaces contact the object from two or more sides, partially enveloping and thus securing it. For example, Choi and Koc recently presented a gripper whose jaws were outfitted with inflatable rubber pockets (15). Earlier, Schmidt (17) and Perovskii (18) introduced the idea of attaching elastic bags loosely filled with granular material, such as small pellets or spheres, to the gripper jaws. A similar idea was also put forward by Rienmüller and Weissmantel (19). These bags conform to the shape of any object they press against and, by simply evacuating the gas inside, can be turned into rigid molds for lifting the object. However, the mechanism for this transformation was not understood and no data about gripping performance were presented. As a result, these early approaches to passive universal grippers never gained traction.

Here we revisit the idea of using granular material for a universal gripper and show that the gripping process is controlled by a reversible jamming transition (20–25). While the concept of jamming has been used to explain the onset of rigidity in a wide range of amorphous systems from molecular glasses to macroscopic granular materials (22, 24, 26), the benefits of jamming for the assembly of materials with tunable behavior are just beginning to be explored. The unique properties of a jamming gripper derive from the fact that loose grains in a bag sit at the threshold between flowing and rigid states (27). This behavior enables the gripper to deform around the target in the unjammed, malleable configuration, then harden when jamming is initiated. In the vicinity of the jamming transition very small modifications of the packing density can drive dramatic changes in the mechanical response (22, 24). Thus, increasing the particle confinement slightly, e.g., by applying a vacuum, enables the gripper to gain remarkable rigidity while almost completely retaining its shape around the target.

We focus on the simplest form of a gripper, a single nonporous elastic bag filled with granular matter (Fig. 1). This system

Author contributions: E.B., J.A., A.M., E.S., M.R.Z., H.L., and H.M.J. designed research; E.B., N.R., J.A., A.M., and E.S. performed research; E.B., N.R., J.A., A.M., E.S., H.L., and H.M.J. analyzed data; and E.B., J.A., and H.M.J. wrote the paper.

Conflict of interest statement: E.B., J.A., H.L., H.M.J., and iRobot Corporation have filed patent applications on related technology.

This article is a PNAS Direct Submission. D.M. is a guest editor invited by the Editorial Board.

[1]To whom correspondence should be addressed. E-mail: embrown@uchicago.edu.

This article contains supporting information online at www.pnas.org/lookup/suppl/doi:10.1073/pnas.1003250107/-/DCSupplemental.

approximates the limit of a robotic hand with infinitely many degrees of freedom, which are actuated passively by contact with the surface of the object to be gripped and are locked in place by a single active element, a pump that evacuates the bag. Fig. 1 demonstrates that a wide range of different types of objects are easily handled in pick-and-place operations using a fixed-base robotic arm, without the need to reconfigure the gripper or even position it precisely, as long as it can cover a fraction of a target object's surface. This adaptability includes switching between objects of different shapes, items difficult to pick up with conventional universal grippers, or fragile targets like raw eggs, as well as simple manipulation tasks, such as pouring water from a glass or drawing with a pen (see Video S1 online). The same type of gripper can also pick up multiple objects simultaneously and deposit them without changing their relative position or orientation. For all of the items depicted in Fig. 1, we find that holding forces can be achieved that exceed significantly the weight of objects of that size. We find that this strength is due to three mechanisms, all controlled by jamming, that can contribute to the gripping process: geometric constraints from interlocking between gripper and object surfaces, static friction from normal stresses at contact, and an additional suction effect, if the gripper membrane can seal off a portion of the object's surface.

Results and Discussion

To evaluate gripping performance we performed pick-and-place operations in which objects were gripped, lifted, and moved (Fig. 1*D*). In addition, the holding forces required to pull out the objects were measured (Fig. 1*E*). These tests were done with a fixed-base robotic arm to which a gripper bag of radius $L = 4.3$ cm was attached, containing ground coffee as the granular material (Fig. 1 *A*–*C*). The bag was filled almost completely but not stretched out so the grains remained loosely packed and the gripper was malleable when no vacuum was applied. By establishing a differential jamming pressure P_{jam} across the bag's latex rubber membrane (0.3 mm in thickness) the packing could be jammed. Employing a Venturi aspirator, compressed air was used to generate pressures P_{jam} around 75 kPa, i.e., the bag was evacuated down to ≈1/4 atm—a level easily reachable with a small vacuum pump. For a wide range of objects, including those shown in Fig. 1 *A* and *E* but also small flashlight light bulbs, M&Ms®, LEDs, bottle caps, plastic tubing, foam ear plugs, and a variety of hardware items and office supplies, the pick-up success rate in 10 trials each was 100%. The magnitude of the holding force, however, was clearly influenced by the objects' shape (Fig. 1*E*). The only objects that could not be gripped were those in which the gripper membrane could not reach sufficiently around the sides, e.g., for hemispheres larger than about half the size of the gripper or for thin disks lying flat, or for very soft objects like cotton balls.

In the following we focus on spheres as test objects to isolate contributions from individual gripping mechanisms and perform quantitative comparisons with model predictions. The gripper used for these holding force measurements was stationary and consisted of a rubber bag (0.3 mm in thickness) with average $L \approx 4$ cm, filled with smooth soda-lime glass spheres 100 μm in diameter to about 80% of the bag volume. The experiment used an inverted configuration, in which the target object, an acrylic sphere with radius R, was attached to an Instron 5869 materials tester and pressed into the gripper bag which itself was fixed to a flat surface. A differential jamming pressure P_{jam} was then applied. The holding strength was measured by pulling the sphere out of the gripper and recording the tensile force as a function of vertical extension. A diagram of this setup and typical force-extension curves for are shown in Fig. 2. Additional measurements showing that the gripper also resists lateral forces as well as torques (required for force closure (10, 15, 28, 29)) are presented in the *SI Text*. The gripping performance was investigated for different P_{jam}, R, and surface properties, although for brevity we focus here on data taken with $P_{\text{jam}} = 80$ kPa and $R = 19$ mm.

Focusing on the maximum force that can be sustained prior to failure, one of the features seen in Fig. 2 is the enhancement of the holding strength when the interface between the sphere and the rubber seals tightly for wet or dry smooth surfaces. This seal is key for the suction effect between the gripper and the sphere. When it cannot be established, shown for the cases of a porous

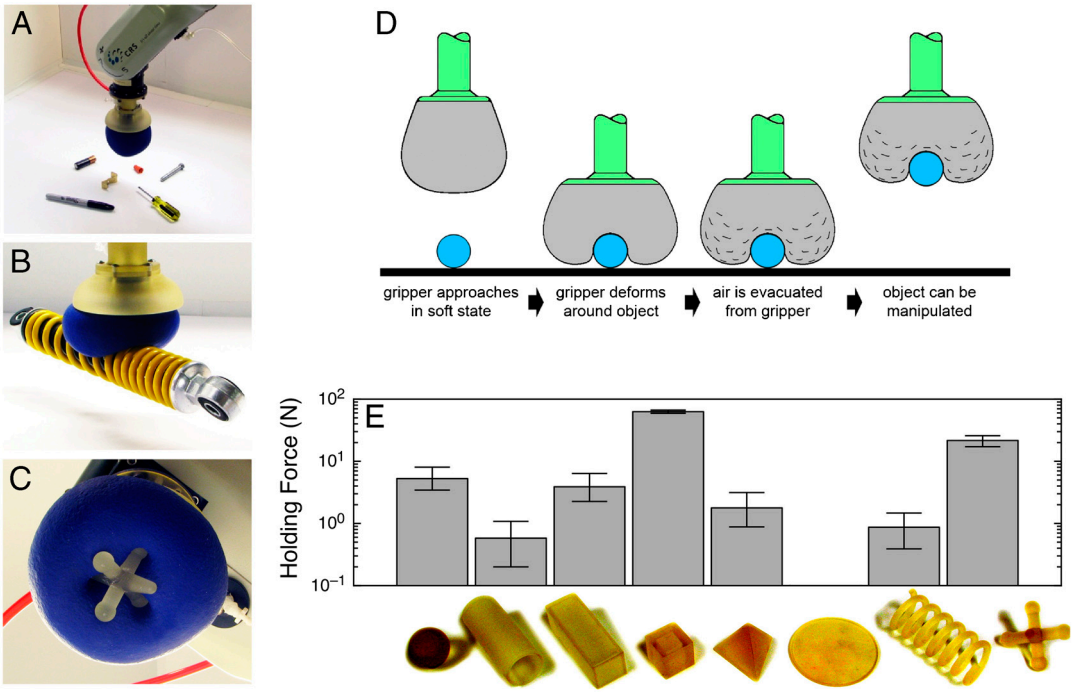

Fig. 1. Jamming-based grippers for picking up a wide range of objects without the need for active feedback. (*A*) Attached to a fixed-base robot arm. (*B*) Picking up a shock absorber coil. (*C*) View from the underside. (*D*) Schematic of operation. (*E*) Holding force F_h for several three-dimensional-printed test shapes (the diameter of the sphere shown on the very left, $2R = 25.4$ mm, can be used for size comparison). The thin disk could not be picked up at all.

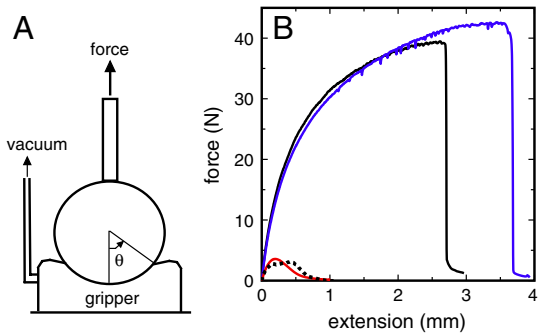

Fig. 2. (*A*): Sketch of setup to measure the holding force. (*B*): Measured force as the sphere is pulled up vertically out of the gripper. Data shown are for fixed contact angle $\theta = \pi/2$, sphere diameter $R = 12.5$ mm, and confining pressure $P_{\text{jam}} = 80$ kPa but different sphere surfaces: solid and dry (black), solid and moistened (blue), solid and powdered with cornstarch (red), porous (dotted). Spheres that form an airtight seal with the gripper membrane are held with a force about 10 times that of porous spheres or those with powdered surfaces that do not seal as well.

sphere or a surface roughened by a coating with ≈20 μm diameter powder particles, the holding force drops significantly.

The degree to which the sphere is enveloped by the gripper is given by the contact angle θ (Fig. 2). Plotting the peak holding force, F_h, as a function of θ, allows us to identify different gripping regimes (Fig. 3 *A*, *B*). Below a minimum angle $\theta \approx \pi/4$ the gripping strength vanishes except for a small contribution from residual membrane stickiness. Above $\pi/4$ there is a rapid increase in F_h with contact angle (red data points). As already seen in Fig. 2, the holding force is enhanced considerably if the sphere surface is smooth to allow for the suction mechanism to operate (black data points). This enhancement occurs with the same onset threshold as for the case without suction. Once the sphere is more than half enveloped and $\theta > \pi/2$, a new regime is entered in which geometric interlocking leads to significant additional holding strength (blue data points).

As the bag is evacuated, the differential pressure P_{jam} across the membrane leads to a volume contraction of the particle packing, as indicated by the sketch in Fig. 3*B*. This contraction has two consequences: it tightens the contact between the bag and the gripped object, and at the same time it jams and hardens the granular material inside the bag. Because the packing density of granular material assembled under gravity is inherently at the threshold of jamming (a pile of grains can sustain a finite angle of repose) even a small applied confining stress P_{jam} can frustrate the ability of grains to slip past one another and drive the packing deep into the jammed state.

For a quantitative modeling of the gripping action, we treat the gripper as an elastic medium and its volume change as producing stresses analogous to differential thermal contraction in a ball-and-socket joint. The contraction of the gripper is expected to pinch the surface of a hard sphere horizontally near the membrane-sphere contact line as sketched in Fig. 3*B*. This pinching applies a stress of magnitude σ^* along a thin band of width δθ centered at θ. We assume that δθ is small and does not vary much with θ. Thus, the pinched region acts like an O-ring of width $d = R\delta\theta$ and diameter $2\pi R \sin\theta$, pressing against the sphere across an area $A_0 = 2\pi R d \sin\theta$. The resulting normal force on the sphere, $F_N = \sigma^* A_0 \sin\theta = 2\pi R d\sigma^* \sin^2\theta$, gives rise to a tangential frictional force of magnitude μF_N where μ is the static coefficient of friction at the membrane/sphere interface. Balancing the vertical components of these forces then gives the maximum vertical force that can be applied before the interface slips, $F_f = F_N(\mu \sin\theta - \cos\theta)$. When the contact angle is less than a critical angle $\theta_c = \arctan(1/\mu)$ then $F_f = 0$ and the interface will slip regardless of the amount of applied normal force. For rubber $\mu \approx 1$ and the contact angle must be greater than about $\pi/4$ for the frictional mechanism to work. For a porous sphere for which a vacuum seal cannot form the holding force thus is

$$F_h = F_f = 2\pi R d\sigma^*(\mu \sin\theta - \cos\theta)\sin^2\theta. \qquad [1]$$

For a smooth solid sphere the effective O-ring can form an airtight seal, which can hold a vacuum in a gap in the region $\pm\theta$ inside the contact line. To show this behavior, we measure the gap pressure P_g inside this region directly by using a sphere with a hole drilled through it and a vacuum gauge attached at the other end. No pressure drop is detected when the gripper contracts around the sphere. This finding demonstrates that the jamming serves the purpose of pinching the membrane to form a seal, but does not by itself generate a vacuum. However, as the sphere is lifted, the jammed material inside the bag deforms, the gap starts to open, and P_g builds up. The resulting vertical suction force is $F_s = P_g A^*$ where A^* is the horizontal cross-sectional area enclosed by the contact line. For a sphere $A^* = \pi R^2 \sin^2\theta$. Fig. 3*C* demonstrates the suction effect in two ways: First, by establishing that an interface pressure P_g is built up as soon as the sphere is

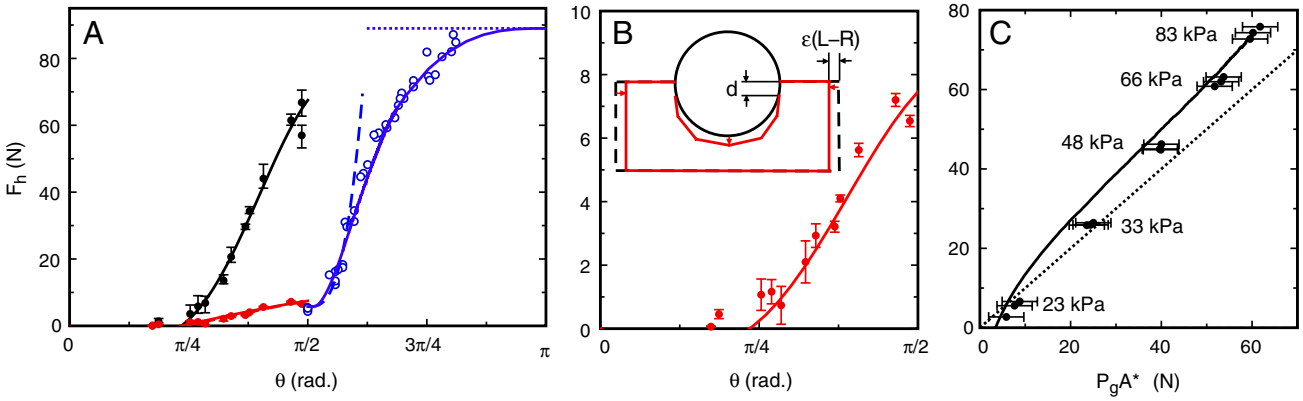

Fig. 3. Gripper holding force F_h. (*A*) F_h as a function of contact angle θ. Data are for a porous sphere gripped by friction for contact angles between $\pi/4$ and $\pi/2$ (red) and by geometrical interlocking for contact angles above $\pi/2$ (blue), and for a solid sphere held by both friction and suction for contact angles between $\pi/4$ and $\pi/2$ (black). Error bars indicate range of forces obtained from five repeated measurements. The uncertainty in θ is 0.05 rad. Lines give predictions as discussed in the text. (*B*) Zoomed-in version of the data in (*A*) for friction. Inset: Sketch of the contraction that occurs when a gripper bag of diameter *L* jams around a sphere, producing an O-ring-like pinching region of width *d* (not to scale). (*C*) Holding force F_h for solid spheres as a function of vacuum pressure P_g in the gap below the sphere, where the gap extends over a horizontal cross-sectional area A^*. (solid line): Build up of P_g during a single run at $P_{\text{jam}} = 80$ kPa in which the sphere was pulled slowly until F_h was reached. (Solid symbols): Maximum holding force F_h in relation to gap pressure P_g for different confining pressures P_{jam} listed on the plot. (dotted line): $F_s = P_g A^*$. All data are for $R = 19$ mm spheres.

pulled on, and second, by showing that the holding force $F_h \propto P_g$ as expected for suction. The dotted line corresponds to $F_s = P_g A^*$, and the excess holding force above this line thus specifies the additional contribution from friction (about 20%).

The pressure on the pinched O-ring will keep the vacuum seal in place as long as the frictional stress exceeds the gap pressure P_g. Thus the maximum gap pressure before the seal fails is $P_g = F_f/A_0 = \sigma^* \sin\theta(\mu \sin\theta - \cos\theta)$. This expression predicts a common onset threshold θ_c for gripping by either friction or suction, as borne out by the data in Fig. 3. As a result, $F_s = P_g A^* = \pi R^2 \sigma^* (\mu \sin\theta - \cos\theta) \sin^3\theta$ and the total holding force combining friction and suction is

$$F_h = F_s + F_f = \pi R^2 \sigma^* (\mu \sin\theta - \cos\theta) \sin^3\theta \left(1 + \frac{2d}{R \sin\theta}\right). \quad [2]$$

Because $A^*/A_0 > 1$, the frictional term, i.e., the second term in the parentheses, typically makes only a small contribution to F_h when a seal is formed.

From simultaneous fits of Eqs. **1** and **2** to the data for the porous and solid spheres, respectively, we find $\mu = 1.04 \pm 0.06$, $\sigma^* = 50 \pm 4$ kPa, and $d = 1.07 \pm 0.07$ mm (these fits extend over the range $\pi/4 < \theta < \pi/2$ in Fig. 3). The fit value for μ is consistent with the independently measured coefficient of friction $\mu = 1.10 \pm 0.03$ (see *Materials and Methods*). This result, along with the fact that $d \ll R$, confirms the assumption that the pinching stress occurs in a thin region near the contact edge in a geometry resembling an O-ring. A simple geometric model for the width of the pinched region on a sphere gives $d = [2\epsilon R(L-R)]^{1/2}$ in the limit $\epsilon \ll 1$ and results in $d = 1.1$ mm, consistent with the fit value. For typical granular materials, confining pressures P_{jam} approaching 1 atm lead to strains ϵ around 1%. Thus, the enhancement of the holding force due to suction is generally expected to be of order $\epsilon^{-1/2} \sim 10$ for spheres. For other target shapes, the seal thickness d will likely depend on the local curvature of the surface it is pressed against, with flatter surfaces allowing for larger values of d.

The contraction stress σ^* can be related to the strength of the jammed state by measuring the compressive strength of the jammed material with a triaxial compression test. A stress-strain curve $\sigma(\epsilon)$ from such a test with a confining pressure $P_{\text{jam}} = 80$ kPa is shown in Fig. 4*A*. To determine which point on the curve is relevant in the gripping experiments, a volumetric strain $\delta V/V$ is measured in the triaxial test cell as the confining pressure is applied. For $P_{\text{jam}} = 80$ kPa, $\delta V/V = -0.004$ as shown in Fig. 4*B*. Note that jamming is a reversible transition and that a similarly minute $\delta V/V$ suffices to drive the packing back into an unjammed configuration. In fact, simply releasing the vacuum (Fig. 4*B*), even without any stirring or jostling, produces significant dilation of the packing and recovery of an easily malleable state. Evaluating the compressive stress in Fig. 4*A* at a linear strain $\epsilon = (1/3)|\delta V/V| = 0.0013$ gives 50 kPa. This result is in excellent agreement with the fit value for σ^*, and thus equates the compressive stress pinching the gripped target with the strength of the jammed material at the strain induced by P_{jam}.

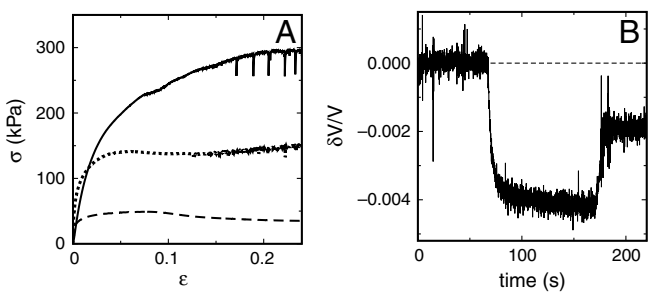

Fig. 4. (*A*) Stress-strain curves σ(ϵ) from triaxial compression (dotted line), triaxial extension (dashed line), and 3-point bending (solid line) tests on 100 μm glass spheres in a latex membrane at $P_{\text{jam}} = 80$ kPa. (*B*) Volumetric strain $\delta V/V$ when a confining stress $P_{\text{jam}} = 80$ kPa is switched on at a time of 65 s and off at 170 s to jam and unjam the gripper.

If the contact angle $\theta > \pi/2$, gripper and gripped object have geometrically interlocked (satisfying form closure, see refs. 15, 28, 29). A gripper with an elastic membrane might conform to protruding parts of objects (as in Fig. 1*C*) to produce such interlocking, but the stiffness of the membrane usually prevents wrapping around convex objects. To investigate the mechanism for interlocking quantitatively and in a simple geometry, we therefore manually molded the jammed gripper around the porous sphere. Then, to break the interlocking effect, the jammed material must both bend out of the way and stretch azimuthally to open enough to let the sphere through. Thus, we expect the holding force in this regime to depend on the resistance to a combination of bending and stretching. Stress-strain curves measured from a 3-point bending test and a triaxial test for extension (stretching) of the granular material are shown in Fig. 4*A*. While these curves differ in some details, they are both characterized by two key features: a linear regime $\sigma = \epsilon E$ in the limit of small strains, where E is the modulus, and at large strains a plateau around a level σ_f, the maximum stress the jammed material can sustain. To understand the interlocking effect we first consider these two limits.

Where there is minimal interlocking, i.e., $\theta - \pi/2 \ll 1$, the strain required to open up the gripper to allow the sphere to escape is small. The minimum contribution from interlocking, F_i, to the holding force is the amount required to bend the ring wrapped around the sphere to vertical so the sphere can slip out. In the small-ϵ limit, $\epsilon \approx 1 - \sin\theta$ and $F_i \approx (\pi/2) E R^2 (t/l)^3 (\theta - \pi/2)^3$, where t is the thickness of the gripper section wrapped around the sphere and l is the bending arm length. Alternatively, to stretch open the neck of the region wrapped around the sphere so it can slip through requires a force $F_i \approx (ERt/6)(\theta - \pi/2)^3$. Because the location of the bend is not predetermined and the thickness is typically nonuniform, these predictions for the scaling can only provide a rough estimate for the magnitude. Because t and l are typically comparable, we take $l \sim t \approx 5$ mm. This simplification gives the same scaling for both bending and stretching. Because the bending resistance is seen to be considerably larger than the resistance to stretching for $\epsilon > 0.003$ (Fig. 4*A*), corresponding to $\theta > 0.53\pi$, bending is expected to dominate the interlocking mechanism at larger θ. The stress-strain curve for bending in Fig. 4*A* is seen to be approximately linear for $\epsilon < 0.02$; by fitting we extract an effective bending modulus $E \approx 7.4$ MPa, and thus $(\pi/2) E R^2 = 4.2$ kN. Fitting $F_h - F_f \propto (\theta - \pi/2)^3$ to the data for $0.53\pi < \theta < 0.57\pi$ in this linear bending-dominated region we obtain the dashed line in Fig. 3*A* and a prefactor $(\pi/2) E R^2 = 1.6 \pm 0.3$ kN. The fact that these two values for the force scale are of the same order of magnitude supports the notion that the initial upturn in holding force for $\theta > \pi/2$ can indeed be attributed to the bending resistance of the jammed material.

In the opposite limit, for a high level of interlocking at large contact angles $\theta \gg \pi/2$, large strains will be required to pry open the bag. In this limit, the plateau of $\sigma(\epsilon)$ at σ_f will cause F_i to saturate for both bending and stretching. The maximum force is then σ_f times a bending area factor, which gives $F_i \sim (2\pi R t^2/l)\sigma_f$. Taking $\sigma_f = 0.29$ MPa from the stress-strain curve for bending (Fig. 4*A*) and $t = l$ leads to $F_i \sim 2\pi R t \sigma_f \approx$ 170 N, about twice the upper limit found in Fig. 3*A* (dotted blue line), again indicating that the scale of the maximum holding force due to interlocking is set by the maximum stress the jammed material can sustain under bending.

To capture the cross-over between these two limits, we use the full stress-strain curve $\sigma(\epsilon)$. Integrating the stress over the bending area gives $F_i = \int_{\pi/2}^{\theta} (2\pi R t^2/l)\sigma(\epsilon) \sin\theta' d\theta'$. The stress can be

evaluated using the small-ϵ limit $\epsilon \approx 1 - \sin\theta$ because that is the only regime where the stress-strain curve is still evolving*. The resulting cross-over is shown as the solid blue line in Fig. 3*A*, scaled by a factor of 0.23 to fit the data.

During operation a grip may experience off-axis forces and torques, in addition to lifting forces discussed so far. We show in the *SI Text* holding forces measured for off-axis forces and torques. We find that the friction mechanism is operative at about the same magnitude for resisting forces in all directions and torques applied at the surface. Suction may be operative in some cases but this is dependent on the target geometry and force direction.

The above results demonstrate that the holding force for all three gripping mechanisms is directly related to the strength of the granular material in its jammed state: contributions to F_h from friction and suction are proportional to the pinching stress σ^* that builds up as the contracting material compresses against the object to be gripped; contributions from geometric interlocking can involve the full stress-strain curve, depending on the extent of interlocking. Because its rigidity is determined by how deep the material is driven into the jammed state by the vacuum-induced volume contraction, the key control parameter for the gripping strength is the confining pressure P_{jam}. In particular, the confining pressure sets the overall scale for the stresses (30) obtained from triaxial compression, 3-point bending, and stretching tests of the granular material as seen in Fig. 4*A*, so σ^* and σ_f are both the same order of magnitude as P_{jam}. Furthermore, the holding forces are approximately proportional to P_{jam} (Fig. 3*C*). While properties of the particles inside the bag such as shape and surface roughness can have a secondary contribution to the stress-strain curves (28) and thus the holding forces, we expect for all three mechanisms the maximum holding force should scale as $F_h \sim P_{\text{jam}} R^2$.

This scaling can be used to estimate the sizes of objects that can be lifted. Because the weight of a gripped object scales with volume, but the holding forces scale with area, we predict that the gripper can pick up objects up to a size of $R_{\text{max}} \sim P_{\text{jam}}/(\rho g)$. For a typical metal ($\rho \approx 10^4$ kg/m^3) and $P_{\text{jam}} \approx 100$ kPa, this relationship gives an upper limit $R_{\text{max}} \sim 1$ m ($\sim 10^4$ kg) with either suction or interlocking. For such big grippers, the weight of the granular material itself might become an issue but can be reduced by using hollow particles. Indeed, meter-size panels of vacuum-packed hollow spheres show remarkable stiffness and have been proposed as structural elements in architectural projects (31–33). While suction is not operative for all objects, interlocking is expected to be prevalent in a multibag, jaw-type gripper (17–19). Still, even without suction or interlocking, friction alone makes it possible to grip and lift solid metal objects up to $R_{\text{max}} \sim 10$ cm. Thus, friction provides more than enough force to pick up any of the objects shown in Fig. 1.

The above analysis was applied to spheres as test objects, but it allows us to draw some general conclusions. For an arbitrarily shaped object, θ can be reinterpreted as the angle of a surface normal vector of the object where the pinching occurs. We can then rewrite Eq. **2** in the form $F_h = \sigma^* \sin\theta(\mu \sin\theta - \cos\theta)[A^* + A_0]$, where it depends only on θ, the pinching area A_0, and the horizontal cross-sectional area A^* inside the pinching perimeter if a seal is formed. Both friction and suction require that the local slope at the contact line be steeper than $\theta_c = \arctan(1/\mu)$.

With this model we can now explain the variation in holding forces measured in Fig. 1*E*. The three-dimensional-printed plastic material in this test is not smooth enough for the gripper to achieve an airtight seal. Thus, the sphere is gripped by friction only and F_h is in the range of what we see in Fig. 2*B* and Fig. 3*A* for porous spheres. The cylinder has a lower F_h compared to a sphere of the same cross-section because it displaces a larger gripper volume which therefore does not reach down as far on the sides, resulting in a smaller vertical component of contact area $A_0 \sin\theta$. Despite its sharp edges, the cube is held with a large force in the range of what is observed for suction with smooth spheres. The flat vertical faces allow for a large contact area from pinching comparable to the area that could be covered by suction, so the frictional effect is about as large as suction. Compared to the cube, the vertical contact area of the cuboid is reduced, just as it is in the comparison between sphere and cylinder. The tetrahedron presents a contact angle $\pi/3$ to the gripper, which explains the slightly reduced F_h compared to the sphere. The flat disk cannot be lifted since the gripper cannot get around the sides; thus the contact angle effectively is zero. The helical spring is similar to the cylinder in shape, and a similar lifting force is found. The jack displays a larger force than can be expected from friction alone, indicating some amount of interlocking, as seen in Fig. 1*C*.

Another aspect concerns the hardness of the object being gripped. So far, we assumed the target was relatively hard so the stress response was solely determined by the gripper hardness. However, for softer targets, the combination of the target and gripper must be considered in series. A soft target will be strained as the gripper contracts, and the pinching pressure at the interface cannot exceed the strain of the gripper under vacuum times the target modulus. Thus, soft targets will experience less holding force. Nevertheless, because friction is more than sufficient to lift hard objects on the cm scale (by a factor of about 30 for a density of 1 g/mL), it should also hold soft targets with a modulus as small as ~1 MPa (about 1/30 of the effective E for compression in (Fig. 4*A*). Indeed, foam earplugs were gripped readily by the setup shown in Fig. 1, but not surprisingly one test object we failed to pick up was a cotton ball.

Neither the bag geometry nor details of the granular material seem to influence F_h strongly, as long as they do not interfere with the degree to which the membrane can conform to an object's surface. In this regard, small grain size will be advantageous. However, very fine powders do not flow well and tend to stick. Furthermore, the gas permeability of a powder scales with the square of the grain diameter (34, 35); thus, decreasing that diameter will increase the pumping time required to reach a strongly jammed state. The membrane itself has to be sufficiently flexible and impermeable to allow for $P_{\text{jam}} > 0$. For friction or suction to work at small contact angles a coefficient of friction $\mu \approx 1$ and some membrane elasticity are desirable, as in a rubbery material, but here we do not focus on optimizing the membrane (see ref. (14) for a discussion of wear resistance of inflatable rubber pockets for robotic grippers). The gripping capabilities are therefore expected to be quite robust.

Conclusions

Our results demonstrate how minute changes in the packing density ($|\delta V/V| < 0.5\%$) associated with a vacuum-induced jamming/unjamming transition enable a universal granular gripper to adapt its shape to a wide range of different objects and pick them up reliably. Without the need for active feedback, this gripper achieves its versatility and remarkable holding strength through a combination of friction, suction, and geometrical interlocking mechanisms. Only a fraction of an object's surface has to be gripped to hold it securely. Applied to spheres as test objects the simple model we introduced captures quantitatively the holding force for all three mechanisms. Specifically, the model relates the gripping performance to the jamming pressure P_{jam} and the stress-strain relationship of the granular material, and it predicts how the holding force scales with object size, surface roughness

*In our gripper the molding of the bag around the test sphere resulted in thinning near the opening, such that t decreased roughly linearly with θ. The effect of such thinning is that F_i levels off at a somewhat lower value and at $\theta < \pi$. To model the thinning, we can take $t \approx 2R(\pi - \theta)/\pi$.

(to the extent that an airtight seal can form), and surface normal angle at the gripper-object interface.

A universal gripper based on jamming may have a variety of applications where some of the high adaptability of a human hand is needed but not available, or where feedback is difficult to obtain or expensive. Examples include situations where very different objects need to be gripped reliably and in rapid succession. A granular system can move with ease from gripping steel springs to raw eggs, and it can pick up and place multiple objects without changing their relative orientation. Its airtight construction also provides the potential for use in wet or volatile environments. Another situation where such a gripper has a significant advantage over traditional designs is when minimal initial information is available, for example when the detailed shape or material properties of the target object are not known a priori, or when precise positioning is not feasible. Because the gripper material adapts and conforms autonomously to the surface of the target object, a jamming-based system can be expected to perform particularly well for complex target shapes.

Materials and Methods

For pick-and-place performance evaluation we used a CRS A465 robotic arm, which includes high-pressure air lines, controlled by an imbedded solenoid valve. Ground coffee was chosen as the grain material for these tests because of its performance in jamming hardness tests. The relatively low density of ground coffee is also advantageous, as it can be used to fill relatively large grippers without weighing them down and straining the membrane. The items shown in Fig. 1*E* were fabricated from photocurable plastic using an Objet three-dimensional printer. For the compressive stress-strain curves and the volumetric strain measurements (Fig. 4) a triaxial test cell (Durham Geo S-510A) was used and the granular material was contained in a 0.6 mm thick cylindrical rubber sleeve (51 mm inner diameter). For bending tests a cylindrical sample 0.3 mm thick with 35.6 mm inner diameter was used in a standard 3-point test fixture. The volumetric strain $\delta V/V$ was obtained by measuring water displacement in the volume surrounding the rubber sleeve while applying vacuum to the interior of the sleeve. The coefficient of friction μ between the acrylic and rubber membrane was obtained by fits to Eqs. **1** and **2** and also measured independently. This measurement was done by an inclined-plane test with four acrylic spheres taped together to prevent rolling on a rubber surface with an applied load of 200 kPa, resulting in $\mu = 1.10 \pm 0.03$. The fact that this value is slightly larger than unity is likely caused by the indentation of the spheres into the soft membrane.

ACKNOWLEDGMENTS. We thank Sid Nagel for insightful discussions and Helen Parks for performing initial tests of the gripping strength. This work was supported by the Defense Sciences Office of the Defense Advanced Research Projects Agency through United States Army Research Office Grant W911NF-08-1-0140. Use of shared experimental facilities supported by the National Science Foundation through the Materials Research Science and Engineering Center (MRSEC) at the University of Chicago is gratefully acknowledged.

1. Pham DT, Yeo SH (1991) Strategies for gripper design and selection in robotic assembly. *Int J Production Res* 29:303–316.
2. Wright PK, Cutkosky MR (1985) *Handbook of ind robotics* (John Wiley & Sons, New York), pp 91–111.
3. Mason MT, Salisbury JK (1985) *Robot hands and the mechanics of manipulation* (MIT Press, Cambridge).
4. Monkman GJ, Hesse S, Steinmann R, Schunk H (2007) *Robot grippers* (Wiley-VCH Verlag GmbH and Co. KGaA, Weinheim).
5. Bicchi A (2000) Hands for dexterous manipulation and robust grasping: A difficult road toward simplicity. *IEEE T Robotic Autom* 16:652–662.
6. Cutkosky MR, Wright PK (1986) Friction, stability, and the design of robotic fingers. *Int J Robotics Res* 5:20–37.
7. Yoshikawa T, Nagai K (1991) Manipulating and grasping forces in manipulation by multifingered robot hands. *IEEE T Robotic Autom* 7:67–77.
8. Park YC, Starr GP (1992) Grasp synthesis of polygonal objects using a 3-fingered robot hand. *Int J Robotics Res* 11:163–184.
9. Chonan S, Jiang ZW, Kosekl M (1996) Soft-handling gripper driven by piezoceramic bimorph strips. *Smart Mater Struct* 5:407–414.
10. Ponce J, Faverjon B (1995) On computing three-finger force-closure grasps of polygonal objects. *IEEE T Robotic Autom* 11:868–881.
11. Buss M, Hashimoto H, Moore JB (1996) Dextrous hand grasping force optimization. *IEEE T Robotic Autom* 12:406–418.
12. Howard WS, Kumar V (1996) On the stability of grasped objects. *IEEE T Robotic Autom* 12:904–917.
13. Dollar AM, Howe RD (2006) A robust compliant grasper via shape deposition manufacturing. *IEEE-ASME Transactions on Mechatronics* 11:154–161.
14. Yokokohji Y, San Martin J, Fujiwara M (2009) Dynamic manipulability of multifingered grasping. *IEEE T Robot* 25:947–954.
15. Choi H, Koc M (2006) Design and feasibility tests of a flexible gripper based on inflatable rubber pockets. *Int J Mach Tool Manu* 46:1350–1361.
16. Hirose S, Umetani Y (1978) Development of soft gripper for the versatile robot hand. *Mechanism and Machine Theory* 13:351–359.
17. Schmidt I (1978) Flexible molding jaws for grippers. *Industrial Robot* 5:24–26.
18. Perovskii AP (1980) Universal grippers for industrial robots. *Russ Eng J* 60:3–4.
19. Rienmüller T, Weissmantel H (1988) A shape adaptive gripper finger for robots. *Proc. 18th International Symposium on Industrial Robots, Lausanne, Switzerland, April 26-28 1988*, ed CW Burckhardt (IFS Publications, Springer Verlag, Berlin), pp 241–250.
20. Majmudar TS, Sperl M, Luding S, Behringer RP (2007) Jamming transition in granular systems. *Phys Rev Lett* 98:058001.
21. Corwin EI, Jaeger HM, Nagel SR (2005) Structural signature of jamming in granular media. *Nature* 435:1075–1078.
22. O'Hern CS, Silbert LE, Liu AJ, Nagel SR (2003) Jamming at zero temperature and zero applied stress: the epitome of disorder. *Phys Rev E* 68:011306.
23. Liu AJ, Nagel SR (2001) *Jamming and rheology : constrained dynamics on microscopic and macroscopic scales* (Taylor & Francis, London).
24. Liu AJ, Nagel SR (1998) Jamming is not just cool any more. *Nature* 396:21–22.
25. Cates ME, Wittmer JP, Bouchaud JP, Claudin P (1998) Jamming, force chains, and fragile matter. *Phys Rev Lett* 81:1841–1844.
26. Trappe V, Prasad V, Cipelletti L, Segre PN, Weitz DA (2001) Jamming phase diagram for attractive particles. *Nature* 411:772–775.
27. Jaeger HM, Nagel SR, Behringer RP (1996) Granular solids, liquids, and gases. *Rev Mod Phys* 68:1259–1273.
28. Murray RM, Li Z, Sastry SS (1994) *A mathematical introduction to robotic manipulation* (CRC Press, Florida).
29. Yoshikawa T (1999) Passive and active closures by constraining mechanisms. *Journal of Dynamic Systems, Measurement and Control* 121:418–424.
30. Lambe TW, Whitman RV (1969) *Soil mechanics* (John Wiley and Sons, New York).
31. Huijben F, van Herwijnen F (2008) Vacuumatics: vacuumatically prestressed (adaptable) structures. *Proc 6th Int Conf Computation of Shell and Spatial Structures IASS-IACM 2008 "Spanning Nano to Mega"*, eds JF Abel and JR Cooke (Multi Science Publishing, United Kingdom).
32. Schmidt T, Lemaitre C, Haase W, Sobek W (2007) Vacuumatics—deflated forms of construction (Vacuumatics—Bauen mit Unterdruck). *Detail* 10:1148–1159.
33. Knaack U, Klein T, Bilow M (2008) *Imagine 02: deflateables* (010 Publishers, Rotterdam, The Netherlands).
34. Möbius ME, et al. (2005) Effect of air on granular size separation in a vibrated granular bed. *Phys Rev E* 72:011304.
35. Pak HK, van Doorn E, Behringer RP (1995) Effects of ambient gases on granular materials under vertical vibration. *Phys Rev Lett* 74:4643–4646.